



The potential of Tanshinone IIA in affecting miR-499-5p/PDCD4 axis in diabetic foot-related endothelial cells

Yu Ming^{1+,B,E-F}, Wei Zhao^{2+,B,E-F}, Bin Cao^{3,A-B,D}, Haiyan Tang^{3,B-D}, Jiuying Ji^{3,B,D-E}, Yongquan Cao^{4,A,C,F}, Shanshan Lu^{5,C,E-F}✉

¹ Institute of Basic Research in Clinical Medicine, China Academy of Chinese Medical Sciences, China

² Pharmacy, Langfang Second People's Hospital, China

³ Traditional Chinese Medicine Dermatology, Hai'an Hospital of Traditional Chinese Medicine, China

⁴ Hai'an Cao Yongquan Dermatology Clinic, China

⁵ Endocrinology, The Affiliated Hospital of Xuzhou Medical University, China

A – Research concept and design, B – Collection and/or assembly of data, C – Data analysis and interpretation, D – Writing the article, E – Critical revision of the article, F – Final approval of the article

* Yu Ming and Wei Zhao contributed equally to the study.

Yu Ming, Wei Zhao, Bin Cao, Haiyan Tang, Jiuying Ji, Yongquan Cao, Shanshan Lu. The Potential of Tanshinone IIA in Affecting miR-499-5p/PDCD4 Axis in Diabetic Foot – Related Endothelial Cells. Ann Agric Environ Med. doi:10.26444/aaem/217674

Abstract

Introduction and Objective. Diabetic foot wound healing is a significant challenge for diabetic patients. Tanshinone IIA (Tan IIA) is widely used in treating diabetes and related complications, but its role in diabetic foot wound healing remains unclear. The aim of the study is to investigate the mechanism of Tan IIA in diabetic foot wound healing.

Materials and Method. Human umbilical vein endothelial cells (HUVECs) cultured in high-glucose medium were used to simulate diabetic pathological conditions. Cell viability and migration were detected by MTT and transwell assays while Annexin V-FITC/PI was used for apoptosis analysis. Measurement of nitric oxide (NO) and Endothelin-1 (ET-1) were performed by ELISA. The expression of vascular endothelial growth factor (VEGF), miR-499-5p and PDCD4 was calculated by RT-qPCR. Dual-luciferase reporter assay was used to validate the interaction of miR-499-5p and PDCD4.

Results. Tan IIA protected high-glucose-treated HUVECs by enhancing cell viability and migration, reducing apoptosis and oxidative stress, and improving endothelial function. Similar effects were observed when miR-499-5p was upregulated. Knockdown of miR-499-5p abolished the protective effects of Tan IIA. PDCD4 was identified as a direct target of miR-499-5p.

Conclusions. Tanshinone IIA protects high glucose-induced HUVECs by enhancing viability, migration, and endothelial function, while reducing apoptosis and oxidative stress, via the miR-499-5p/PDCD4 axis. These *in vitro* findings support its potential in diabetic foot wound healing, pending *in vivo* validation.

Key words

wound healing, miR-499-5p, diabetic foot, Tanshinone IIA

INTRODUCTION

Diabetic foot is a severe complication of diabetes which can lead to gangrene [1], and even amputation [2] in severe cases. Persistent hyperglycaemia can drive oxidative stress and inflammation, sequentially causing endothelial injury and neuropathy that cause recalcitrant ulcers [3, 4]. In clinical settings, although vasodilators and anticoagulants are commonly used to enhance blood flow, their application is limited to adverse reactions, prolonged treatment period, and inconsistent efficacy [5].

Traditional Chinese medicine is characterized by dual internal and external usage which also exerts effects in enhancing local oxygen supply and suppressing inflammatory cytokines [6]. Tanshinone IIA (Tan IIA) exerts extensive protective effects against diabetes and various associated complications. Existing studies indicate that Tan IIA exhibits a significant protective effect in diabetic nephropathy by inhibiting inflammatory responses [7] and oxidative

stress [8]. Findings also confirm that it plays a regulatory role in angiogenesis in patients with hyperglycaemia [9]. Additionally, Tan IIA has the function of protecting vascular endothelial cells [10]. Therefore, it is speculated that Tan IIA holds the potential for promoting wound healing in diabetic foot, although the underlying mechanism remains to be elucidated.

Previous research has substantiated the remarkable role of microRNAs (miRNAs) in facilitating wound healing of diabetic foot; for instance, miR-31-5p expedites diabetic wound healing by boosting angiogenesis [11]. Additionally, miRNAs are capable of modulating the expression of angiogenesis-related genes and can stimulate the proliferation, migration and lumen formation of vascular endothelial cells, thereby exerting an impact on wound angiogenesis [12].

Based on current reports, miR-499-5p has been found to have a close link with cell damage; for instance, miR-499-5p mitigates myocardial cell damage by reducing apoptosis and oxidative stress [13]. Findings from the atherosclerotic cell model indicate that miR-499-5p/SOX6 regulates angiogenesis by affecting the proliferation and migration of vascular smooth muscle cells [14]. Moreover, in diabetic cardiomyopathy, the up-regulated miR-499-5p

✉ Address for correspondence: Shanshan Lu, Endocrinology, The Affiliated Hospital of Xuzhou Medical University, China
E-mail: lushanshaner@163.com

has been proven to mitigate cardiac diastolic dysfunction [15]. These findings suggest a potential association between the expression of miR-499-5p and diabetic wound healing.

The aim of this is to investigate whether Tan IIA promotes wound healing in diabetic foot by regulating miR-499-5p and its downstream targets in HUVECs.

MATERIALS AND METHOD

Stock solution of Tan IIA. Tan IIA (2.3 mg) was completely dissolved into 78.0 μ L DMSO, following which stock solution at 100 mM was obtained and stored at -20°C for later use.

Cell culture and transfection. The commercialized HUVECs were seeded in DMEM (Thermo Fischer) with 10% FBS. The normal glucose group (NG) was cultured in DMEM with 5.5mM glucose and the high glucose group (HG) was with 33 mM glucose. Cells with confluency up to 70% were applied for transient transfection of miR-499-5p mimic and mimic NC, miR-499-5p inhibitor and inhibitor NC, by Lipofectamine 3000. During the transfection process, both FBS and antibiotics-free medium were necessary. The cells in each well of 24-well plate was about 1×10^5 . In addition, for Tan IIA treatment, the final concentration of DMSO did not exceed 0.1% [16]. The final concentration of miR-499-5p mimic or inhibitor was 50 nM, respectively, for each well of 24-well plate. RT-qPCR was used to detect the expression level of miR-499-5p after transfection to validate the transfection efficiency. The background values were subtracted and results expressed as a percentage of the negative-control group ($n = 3$ independent experiments, each in triplicate).

Cell viability. Viability was measured via the CCK-8 kit. HUVECs were seeded in a 96-well plate with 8,000 per well and cultured overnight before Tan IIA treatment or transfection. CCK-8 solution was then added and mixed gently in each well and the plate incubated for 2h at dark. Absorbance at 450nm was detected with a microplate reader. The background values were subtracted, and results expressed as percentage of the negative-control group. Three repetitions were performed for each experiment.

Cell migration. The migration ability was assessed by transwell assay, HUVECs were suspended in DMEM with a density of $1 \times 10^5/\text{mL}$. The upper chamber was filled with 200 μ L cell suspension while 500 μ L complete medium was added to the lower chamber. Migrated cells 24 h later were fixed with 4% PFA for 15 min and stained with 0.1% crystal violet for 20 min. Cell numbers were calculated by microscope. Five random fields were photographed and cells were counted.

Cell apoptosis. The apoptosis rate of HUVECs after various treatments was detected by Annexin V-FITC/PI kit. Collected HUVECs were washed in ice-cold PBS ($1 \times$) at least twice. Subsequently, Annexin V-FITC at 0.5 $\mu\text{g}/\text{mL}$ along with PI at 50 $\mu\text{g}/\text{mL}$ were added and for 15 min. The apoptosis rate was analyzed by flow cytometer. For sample analysis, debris was first excluded by FSC/SSC gating. Then, Annexin V-FITC versus PI plots were employed to define early (Annexin V⁺/PI⁻) and late (Annexin V⁺/PI⁺) apoptotic cells. Total apoptosis was reported as the sum of both populations.

NO and ET-1 detection. The nitric oxide (NO) and Endothelin-1 (ET-1) contents in cell supernatant were determined by ELISA assay. After various treatments, the culture medium was collected for subsequent experiments. All procedures were performed in strict accordance with instructions. Absorbance was analyzed by a microplate reader.

SOD and MDA detection. The measurement of superoxide dismutase (SOD) activity in HUVECs was accomplished by SOD assay kit (Sangong). Following the specifications, HUVECs were lysed in SOD working solution and incubated for 0.5 h at a constant temperature of 37°C . The content of malondialdehyde acid (MDA) was also detected by a corresponding kit (Solarbio). HUVECs were lysed in RIPA and mixed with the working solution containing thiobarbituric acid. All samples were then placed in boiled water for 5 min. The supernatant of cell lysis products was applied for content detection. Detection of SOD activity and MDA content was carried out by a microplate reader.

Dual-luciferase reporter assay. The 3'UTR of PDCD4 (WT-PDCD4), including predictive interaction sites with miR-499-5p and its mutant (MUT-PDCD4), were separately inserted into the pmirGL3 vector. The recombined vector was transfected into HUVECs with miR-499-5p mimic (Mimic NC as the negative control), miR-499-5p inhibitor (Inhibitor NC as the negative control). The luciferase activity was calculated in comparison with the control 48h later.

RT-qPCR. RNA was isolated from HUVECs with Trizol (Invitrogen) under the guidance of specifications. Isolated RNA was then transcribed into cDNAs by reverse transcription kit, and placed at -20°C for storage. The expression level of miR-499-5p, vascular endothelial growth factor (VEGF) and PDCD4 were estimated by a SYBR Green PCR kit. For qPCR, U6 as well as GAPDH were used as the internal reference, while data was processed by the $2^{-\Delta\Delta\text{CT}}$ method.

Statistical analysis. Data was processed using GraphPad Prism 7.0. All experiments were independently repeated at least 3 times with 3 technical replicates each. Normality was verified by the Shapiro-Wilk test, and variance homogeneity by Levene's test. Multiple group comparisons were performed using one-way ANOVA, followed by Tukey's HSD *post-hoc* test for pairwise comparisons. Statistical significance was defined as $P < 0.05$. The sample size was estimated by the G*Power 3.1, $\alpha = 0.05$, power = 0.80. G*Power 3.1 indicated that 3 independent experiments (each with 3 technical replicates) were sufficient. Data were collected from 3 independent biological replicates, with each run in triplicate (technical replicates), and presented as mean \pm SD.

RESULTS

Tan IIA protects high-glucose-treated HUVECs. To determine the optimal concentration, HUVECs under high-glucose conditions were treated with various concentrations of Tan IIA for 24 h. The high glucose reduced cell viability to 60% of NG and 20 $\mu\text{g}/\text{mL}$ Tan IIA restored it to 81% of the normal level (Fig. 1A; $P < 0.01$). The 20 $\mu\text{g}/\text{mL}$ Tan IIA was used in subsequent experiments. Similarly, migrated cells

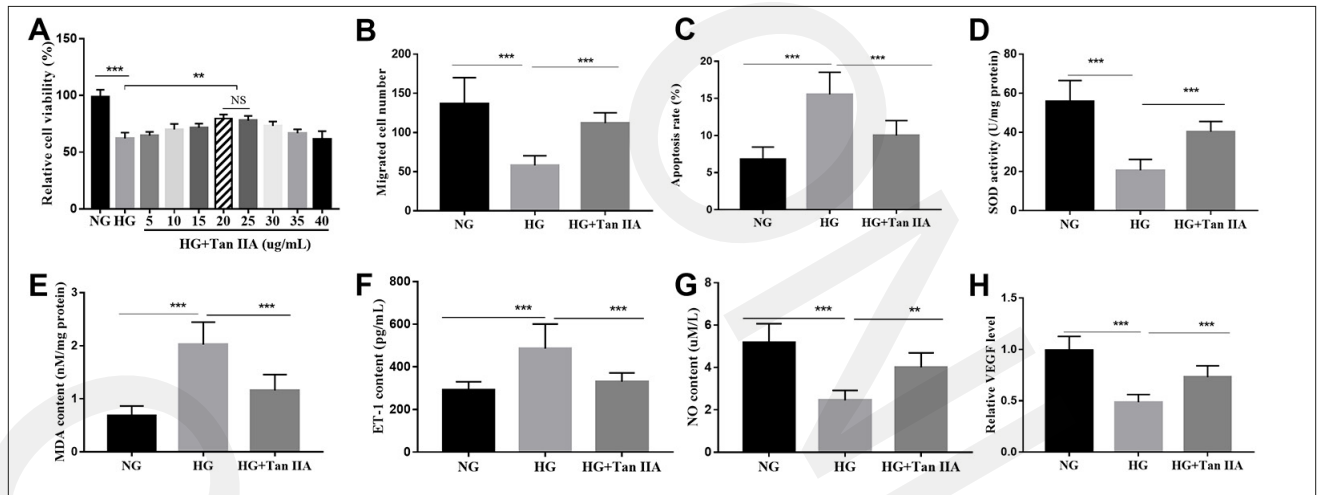


Figure 1. Protective effects of Tan IIA on HUVECs treated with high-glucose. (A-C) Effect of tanshinone IIA (Tan IIA) at different concentrations ($\mu\text{g/mL}$) on HUVECs viability, migration and apoptosis. (D) Effect of Tan IIA on SOD activity in HUVECs. (E) Effect of Tan IIA on MDA content in HUVECs. (F) Effect of Tan IIA on ET-1 content in the supernatant. (G) Effect of Tan IIA on NO content in the supernatant. (H) Effect of Tan IIA on the relative expression level of VEGF. *** $P < 0.001$; ** $P < 0.01$.

were reduced to 43% of NG under HG conditions, while Tan IIA improved it to 82% (Fig. 1B; $P < 0.001$). Apoptosis increased 2-fold under HG conditions, but was reduced to 1.4-fold of NG by Tan IIA (Fig. 1C; $P < 0.001$). High-glucose exposure decreased SOD activity to 36%, whereas supplementation with Tan IIA restored activity to 72% of the NG level (Fig. 1D; $P < 0.001$). The high-glucose treatment increased MDA levels 3-fold compared to NG, whereas Tan IIA reduced this elevation to 1.5-fold (Fig. 1E; $P < 0.001$). Furthermore, high-glucose treatment increased ET-1 content by 1.7-fold, an effect that was mitigated by Tan IIA to near-basal levels (Fig. 1F; $P < 0.001$). Moreover, high-glucose treatment decreased the NO content by 50%, and Tan IIA administration successfully restored 80% of the original content (Fig. 1G; $P < 0.001$). Finally, high-glucose reduced VEGF mRNA to 42% of NG, and Tan IIA restored it to 80% of normal levels (Fig. 1H; $P < 0.001$). These findings highlighted the potential restorative properties of Tan IIA.

miR-499-5p expression in high-glucose-treated HUVECs.

To explore the potential association between miR-499-5p and the wound healing of diabetic foot, the expression level of miR-499-5p was initially measured in HUVECs, both before and after high-glucose treatment. The obtained experimental data manifested that the miR-499-5p level was decreased by 54% following high-glucose treatment (Fig. 2; $P < 0.001$). The expression level of miR-499-5p under different concentrations of Tan IIA was also compared. Results revealed that the decreased miR-499-5p could be reverted to 81% of normal levels by the supplement with Tan IIA at 20 $\mu\text{g/mL}$ (Fig. 2; $P < 0.001$).

Effect of miR-499-5p on HUVECs treated with high-glucose.

As the above findings confirmed the prominent decrease of miR-499-5p in HUVECs treated with high-glucose, the underlying effects of highly expressed miR-499-5p on the functions of endothelial cells were investigated. The relative miR-499-5p level was confirmed by RT-qPCR (Fig. 3A; $P < 0.001$). Under the conditions induced by high glucose, the viability and migration of HUVECs exhibited a decline of approximately 50% (Fig. 3B-C; $P < 0.001$), accompanied by an elevated apoptosis of 3 times (Fig. 3D;

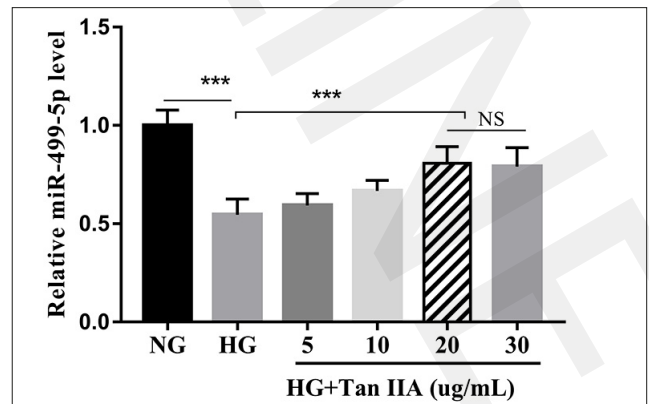


Figure 2. Relative expression level of miR-499-5p in HUVECs treated with high glucose and Tan IIA of various concentrations. *** $P < 0.001$.

$P < 0.001$). Intriguingly, these detrimental effects were notably mitigated by the application of the miR-499-5p mimic with a restoration of 82% of its original level in viability and migration, and 59% reduction for elevated apoptosis (Fig. 3B-D; $P < 0.001$). Furthermore, the baleful oxidative stress with suppressed SOD activity (30% of NG) and increased MDA level (3-fold of NG) was also distinctly reversed by miR-499-5p mimic (Fig. 3E-F; $P < 0.001$). The evaluation of vascular endothelial cell function revealed that exposure to high glucose led to 60% elevation in ET-1 and a 50% decline in NO (Fig. 3G-H; $P < 0.01$). Remarkably, the up-regulation of miR-499-5p effectively counteracted these adverse alterations (Fig. 3G-H; $P < 0.05$). Besides, the VEGF mRNA level exhibited 49% decrease after high-glucose treatment compared to the NG group, which was improved to nearly 84% of the normal level by miR-499-5p mimic (Fig. 3I; $P < 0.001$).

The above results demonstrated the ameliorative effect of elevated miR-499-5p on the function of endothelial cells.

miR-499-5p knockdown abolishes the effects of Tan IIA.

To confirm whether Tan IIA exerted its protective effect via miR-499-5p, miR-499-5p was knockdown by transfection of miR-499-5p inhibitor in HUVECs treated with high-glucose and Tan IIA. A comprehensive evaluation

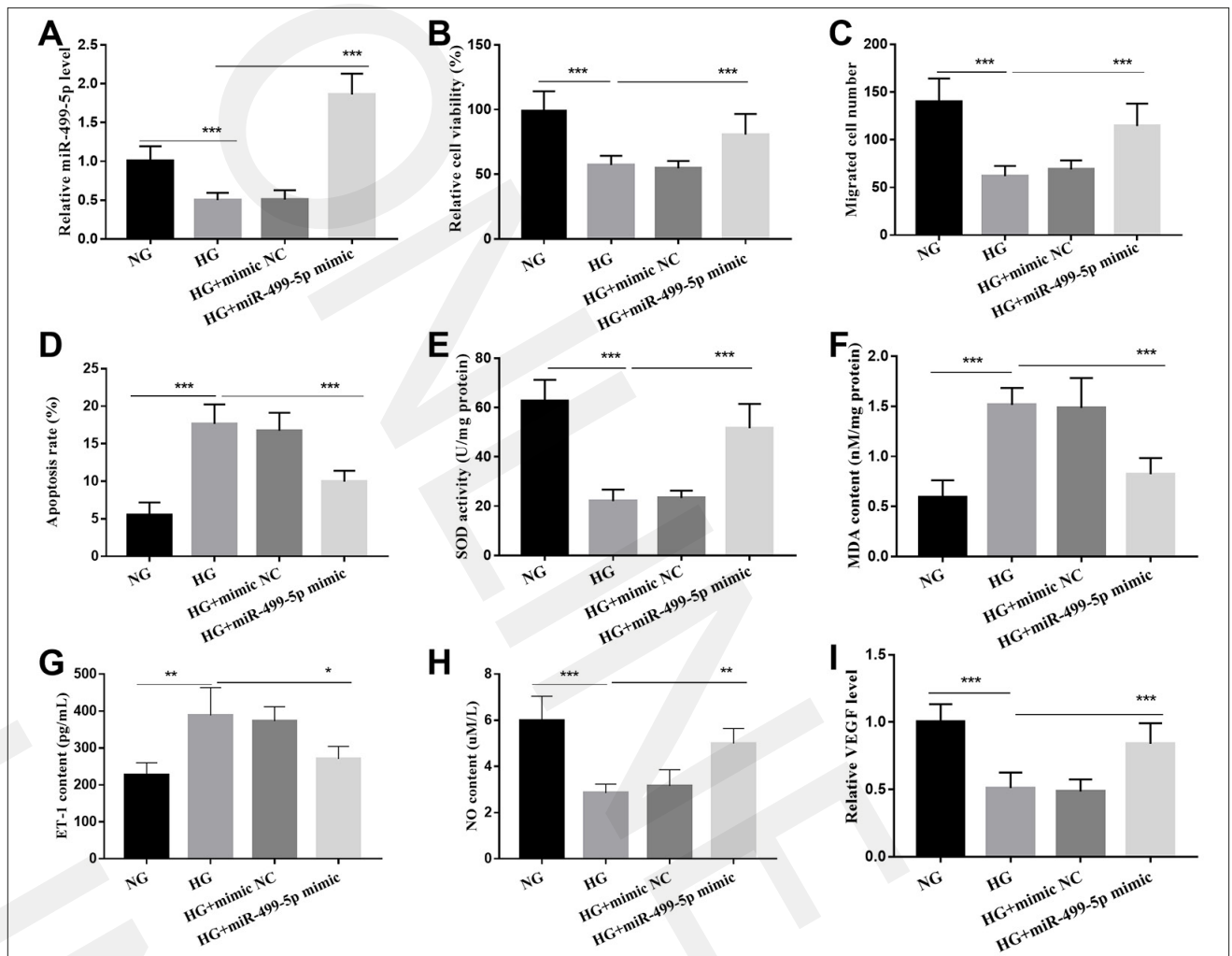


Figure 3. Effect of elevated miR-499-5p on HUVECs treated with high-glucose. (A) Relative miR-499-5p level in HUVECs treated with high glucose and transfection with miR-499-5p mimic. (B–D) Effect of elevated miR-499-5p on cell viability, migration and apoptosis. (E) Effect of elevated miR-499-5p on SOD activity. (F) Effect of elevated miR-499-5p on MDA content. (G) Effect of elevated miR-499-5p on ET-1 content in the supernatant. (H) Effect of elevated miR-499-5p on NO content. (I) Effect of elevated miR-499-5p on the relative expression level of VEGF. *** $P < 0.001$, ** $P < 0.01$.

of HUVECs function was also carried out. In HUVECs induced by high glucose, Tan IIA elevated the level of miR-499-5p by about 79% of the normal level. Nevertheless, this upward trend was then negated by subsequent introduction of the miR-499-5p inhibitor, reaching 46% of NG group (Fig. 4A; $P < 0.001$). Similarly, the ameliorative effects of 80% restoration on cell proliferation and migration by Tan IIA, were also nullified to approximately one-half by subsequent miR-499-5p knockdown (Fig. 4B–C; $P < 0.01$). Although Tan IIA supplement effectively decreased the apoptosis rate from 2.6-fold to 1.3-fold, the miR-499-5p inhibitor negated this beneficial effect, leading to a more than 2-fold apoptosis rate (Fig. 4D; $P < 0.01$).

Assessment of oxidative stress markers revealed that Tan IIA contributed significantly to boosting the activity of SOD from 30% to 63% of the normal level, and decreasing the content of MDA from 3.8-fold to 1.5-fold of NG group (Fig. 4E–F; $P < 0.001$). However, the antioxidant effects of Tan IIA were obliterated by transient cell transfection of miR-499-5p inhibitor, and SOD activity reached 18.8% of the original level, with 3-fold elevation in MDA content (Fig. 4E–F; $P < 0.001$). Tan IIA also exhibited beneficial effects in improving endothelial cell function, including reducing the

content of ET-1 to nearly normal level and increasing the content of NO to 84% of the NG group. Nevertheless, these effects were counteracted by miR-499-5p inhibitor, with ET-1 increased to 1.5-fold and NO decreased to 55.6% compared to the normal (Fig. 4G–H; $P < 0.01$). The suppressive effect of miR-499-5p inhibitor was also manifested in countering the promotion of VEGF expression level by Tan IIA. Briefly, Tan IIA can restore the suppressed VEGF mRNA to 74% of the NG level, which was then decreased to 41% by the miR-499-5p inhibitor (Fig. 4I; $P < 0.001$). Collectively, miR-499-5p knockdown exacerbated the endothelial cell damage and effectively counteracted the protective effects of Tan IIA in HUVECs treated with high glucose. Tan IIA might exert its improvement effect in promoting diabetic foot wound healing by regulating the expression level of miR-499-5p.

PDCD4 was a potential target of miR-499-5p. To elucidate the role of miR-499-5p in pathologically altered HUVECs, the prediction of a downstream target was performed in the ENCORI database. Notably, the results indicated that PDCD4 was a potential target of miR-499-5p (Fig. 5A), which was validated in the dual-luciferase reporter system. The luciferase activity was affected by the co-transfection of miR-499-5p

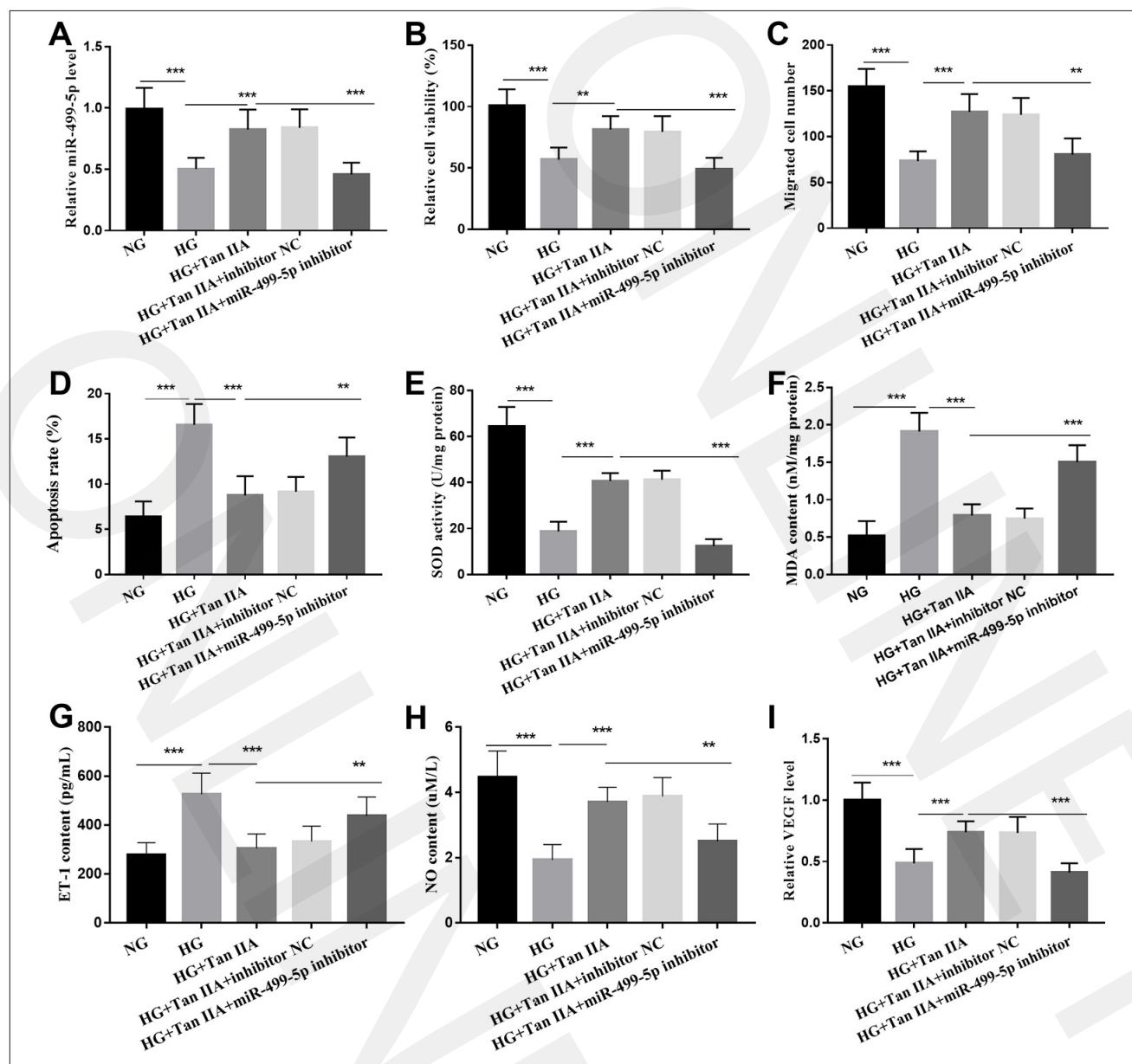


Figure 4. miR-499-5p knockdown suppressed the protective effects of Tan IIA on HUVECs treated with high glucose. (A) Relative miR-499-5p level after knockdown in HUVECs treated with high glucose and Tan IIA. (B-D) Measurement on cell viability, migration and apoptosis of HUVECs. (E) Detection on SOD activity. (F) Assessment of MDA content. (G) Detection on ET-1 content in the supernatant. (H) analysis on NO content in the supernatant. (I) Relative expression level of VEGF. *** $P < 0.001$, ** $P < 0.01$.

mimic or inhibitor and WT-PDCD4 (Fig. 5B; $P < 0.001$) instead of the MUT-PDCD4 (Fig. 5C). The expression level of PDCD4 in HUVECs was also measured based on elevating or reducing the miR-499-5p level. Quantitative analysis confirmed that the PDCD4 level significantly declined in response to the transfection of miR-499-5p mimic, and conversely, the expression of PDCD4 was distinctly elevated with the knockdown of miR-499-5p (Fig. 5D; $P < 0.001$). These findings indicated a negative interaction between miR-499-5p and PDCD4.

DISCUSSION

Diabetic foot is a serious complication of diabetes, with complex pathogenesis [17]. Although in recent years various drugs have been applied for the treatment of diabetic foot

wound, their effects remain limited and diabetic patients still face the challenge of delayed wound healing [18].

The present study demonstrates that Tan IIA exerts protective effects on high glucose-induced HUVECs through the miR-499-5p/PDCD4 axis, as evidenced by enhanced cell viability, migration, reduced apoptosis, alleviated oxidative stress, and improved endothelial function (e.g., upregulated NO and VEGF, downregulated ET-1). These findings provide preliminary *in vitro* evidence for the potential role of Tan IIA in diabetic foot wound healing, particularly in regulating endothelial cell function – a key process in angiogenesis and wound revascularization.

Reports from diabetic rat models and HUVECs induced by high glucose confirmed that Tan II enhanced endothelial nitric oxide synthase (eNOS) expression and NO production, thus improving endothelial-dependent vascular dysfunction [19], demonstrating its potential for treating

5p has been proven to alleviate oxidative stress and apoptosis in cardiovascular and metabolic diseases, and PDCD4 is a known regulator of cell survival and inflammation in diabetes, the results of the presented study first suggest that targeted therapy of miR-499-5p/PDCD4 axis may be a promising strategy to improve endothelial dysfunction in diabetic foot.

Further research by the authors of the current study indicated that in HUVECs treated by high glucose, miR-499-5p knockdown apparently nullified the ameliorative effect of Tan II. The authors' prediction and validation in dual-luciferase system verified that PDCD4 was a direct target of miR-499-5p, which has also been reported elsewhere [30]. Currently, abundant literature has firmly established that PDCD4 is considered as a novel therapeutic target for metabolic disorders, such as obesity and diabetes, which are associated with oxidative stress, chronic inflammation, as well as insulin resistance [31]. Research has shown that PDCD4 exerts a pronounced pro-inflammatory effect [32], and its deficiency can alleviate insulin resistance by suppressing cell apoptosis and inflammation in the type 2 diabetic model [33]. Results from the cell models of diabetic foot wound healing have verified the abnormal up-regulation of PDCD4 [34] which is consistent with the results of the current study. Supportive findings from prior reports can account for this outcome. For instance, promoting angiogenesis is achieved by downregulating rather than enhancing PDCD4 [35, 36]. Additionally, research on diabetic cardiomyopathy has demonstrated that elevating PDCD4 expression promotes cell apoptosis [37]. Thus, the highly expressed PDCD4 may inhibit wound healing in HUVECs treated with high glucose, by promoting apoptosis and oxidative stress, and suppressing cell proliferation and angiogenesis.

Limitations of the study. It should be noted the study has limitations. It was initially found that Tan IIA protects high-glucose-exposed HUVECs by boosting viability, attenuating apoptosis and oxidative stress through the miR-499-5p/PDCD4 axis. For instance, the findings are confined to an *in vitro* HUVEC model and await validation in animal or human models. However, the Tan IIA concentrations used may not be attainable *in vivo*, therefore the data cannot qualify Tan IIA as a therapeutic option for diabetic foot ulcers.

CONCLUSION

Tan IIA protects high-glucose-injured endothelial cells via miR-499-5p/PDCD4, offering an *in vitro* rationale for evaluating Tan IIA formulations in diabetic wound models. Future research should establish dose–response relationships *in vivo* and explore additional miRNAs that cooperate with miR-499-5p.

Funding

The study was funded by the National Major S & T Special Project for Significant New Drugs Development (Special Project No. 2017ZX09301059).

REFERENCES

- Korzon-Burakowska A, Dziemidok P. Diabetic foot – the need for comprehensive multidisciplinary approach. *Ann Agric Environ Med*. 2011;18(2):314–7.
- Sanchez ML, Valdez H, Conde M, et al. Polymers and Bioactive Compounds with a Macrophage Modulation Effect for the Rational Design of Hydrogels for Skin Regeneration. *Pharmaceutics*. 2023;15(6).
- Volmer-Thole M, Lobmann R. Neuropathy and Diabetic Foot Syndrome. *Int J Mol Sci*. 2016;17(6).
- Bus SA, Lavery LA, Monteiro-Soares M, et al. Guidelines on the prevention of foot ulcers in persons with diabetes (IWGDF 2019 update). *Diabetes Metab Res Rev*. 2020;36 Suppl 1:e3269.
- Everett E, Mathioudakis N. Update on management of diabetic foot ulcers. *Ann N Y Acad Sci*. 2018;1411(1):153–65.
- Liu Y, Mo J, Liang F, et al. Pien-tze-huang promotes wound healing in streptozotocin-induced diabetes models associated with improving oxidative stress via the Nrf2/ARE pathway. *Front Pharmacol*. 2023;14:1062664.
- Xu Z, Cai K, Su SL, et al. Salvianolic acid B and tanshinone IIA synergistically improve early diabetic nephropathy through regulating PI3K/Akt/NF- κ B signaling pathway. *J Ethnopharmacol*. 2024;319(Pt 3):117356.
- Wu Q, Guan YB, Zhang KJ, et al. Tanshinone IIA mediates protection from diabetes kidney disease by inhibiting oxidative stress induced pyroptosis. *J Ethnopharmacol*. 2023;316:116667.
- Chen L, He W, Peng B, et al. Sodium Tanshinone IIA sulfonate improves post-ischemic angiogenesis in hyperglycemia. *Biochem Biophys Res Commun*. 2019;520(3):580–5.
- Zhu J, Chen H, Guo J, et al. Sodium Tanshinone IIA Sulfonate Inhibits Vascular Endothelial Cell Pyroptosis via the AMPK Signaling Pathway in Atherosclerosis. *J Inflamm Res*. 2022;15:6293–306.
- Yan C, Chen J, Wang C, et al. Milk exosomes-mediated miR-31-5p delivery accelerates diabetic wound healing through promoting angiogenesis. *Drug Deliv*. 2022;29(1):214–28.
- Ozdemir D, Feinberg MW. MicroRNAs in diabetic wound healing: Pathophysiology and therapeutic opportunities. *Trends Cardiovasc Med*. 2019;29(3):131–7.
- Sun S, Ruan Y, Yan M, et al. Ferulic Acid Alleviates Oxidative Stress-Induced Cardiomyocyte Injury by the Regulation of miR-499-5p/p21 Signal Cascade. *Evid Based Complement Alternat Med*. 2021;2021:1921457.
- Sheng Y, Yang Z, Feng Z, et al. MicroRNA-499-5p promotes vascular smooth muscle cell proliferation and migration via inhibiting SOX6. *Physiol Genomics*. 2023;55(2):67–74.
- Zhao L, Li W, Zhao H. Inhibition of long non-coding RNA TUG1 protects against diabetic cardiomyopathy induced diastolic dysfunction by regulating miR-499-5p. *Am J Transl Res*. 2020;12(3):718–30.
- Zhu H, Chen Z, Ma Z, et al. Tanshinone IIA Protects Endothelial Cells from H₂O₂-Induced Injuries via PXR Activation. *Biomolecules & Therapeutics*. 2017;25(6):599–608.
- Johansen OE, Birkeland KI, Jorgensen AP, et al. Diabetic foot ulcer burden may be modified by high-dose atorvastatin: A 6-month randomized controlled pilot trial. *J Diabetes*. 2009;1(3):182–7.
- Li Y, Wang X, Chen J, et al. Structural analysis and accelerating wound healing function of a novel galactosylated glycosaminoglycan from the snail *Helix lucorum*. *Carbohydr Polym*. 2025;348(Pt B):122900.
- Li YH, Xu Q, Xu WH, et al. Mechanisms of protection against diabetes-induced impairment of endothelium-dependent vasorelaxation by Tanshinone IIA. *Biochim Biophys Acta*. 2015;1850(4):813–23.
- Liu B, Liu L, Zang A, et al. Tanshinone IIA inhibits proliferation and induces apoptosis of human nasopharyngeal carcinoma cells via p53-cyclin B1/CDC2. *Oncol Lett*. 2019;18(3):3317–22.
- Nie ZY, Zhao MH, Cheng BQ, et al. Tanshinone IIA regulates human AML cell proliferation, cell cycle, and apoptosis through miR-497-5p/AKT3 axis. *Cancer Cell Int*. 2020;20:379.
- Zhang L, Yang F. Tanshinone IIA improves diabetes-induced renal fibrosis by regulating the miR-34-5p/Notch1 axis. *Food Sci Nutr*. 2022;10(11):4019–40.
- Yang C, Mu Y, Li S, et al. Tanshinone IIA: a Chinese herbal ingredient for the treatment of atherosclerosis. *Front Pharmacol*. 2023;14:1321880.
- Lu TC, Wu YH, Chen WY, Hung YC. Targeting Oxidative Stress and Endothelial Dysfunction Using Tanshinone IIA for the Treatment of Tissue Inflammation and Fibrosis. *Oxid Med Cell Longev*. 2022;2022:2811789.

25. Chen L, Guo QH, Chang Y, et al. Tanshinone IIA ameliorated endothelial dysfunction in rats with chronic intermittent hypoxia. *Cardiovasc Pathol*. 2017;31:47–53.
26. Qin C, Liu S, Zhou S, et al. Tanshinone IIA promotes vascular normalization and boosts Sorafenib's anti-hepatoma activity via modulating the PI3K-AKT pathway. *Front Pharmacol*. 2023;14:1189532.
27. Han D, Wu X, Liu L, et al. Sodium tanshinone IIA sulfonate protects ARPE-19 cells against oxidative stress by inhibiting autophagy and apoptosis. *Sci Rep*. 2018;8(1):15137.
28. Yang JX, Pan YY, Ge JH, et al. Tanshinone II A Attenuates TNF- α -Induced Expression of VCAM-1 and ICAM-1 in Endothelial Progenitor Cells by Blocking Activation of NF- κ B. *Cell Physiol Biochem*. 2016;40(1–2):195–206.
29. Wang X, Wu C. Tanshinone IIA improves cardiac function via regulating miR-499-5p dependent angiogenesis in myocardial ischemic mice. *Microvasc Res*. 2022;143:104399.
30. Li Y, Lu J, Bao X, et al. MiR-499-5p protects cardiomyocytes against ischaemic injury via anti-apoptosis by targeting PDCD4. *Oncotarget*. 2016;7(24):35607–17.
31. Lu K, Chen Q, Li M, et al. Programmed cell death factor 4 (PDCD4), a novel therapy target for metabolic diseases besides cancer. *Free Radic Biol Med*. 2020;159:150–63.
32. Merline R, Moreth K, Beckmann J, et al. Signaling by the matrix proteoglycan decorin controls inflammation and cancer through PDCD4 and MicroRNA-21. *Sci Signal*. 2011;4(199):ra75.
33. Zhang J, Zhang M, Yang Z, et al. PDCD4 deficiency ameliorates left ventricular remodeling and insulin resistance in a rat model of type 2 diabetic cardiomyopathy. *BMJ Open Diabetes Res Care*. 2020;8(1).
34. Li T, Ma Y, Wang M, et al. Platelet-rich plasma plays an antibacterial, anti-inflammatory and cell proliferation-promoting role in an in vitro model for diabetic infected wounds. *Infect Drug Resist*. 2019;12:297–309.
35. Pin G, Huanting L, Chengzhan Z, et al. Down-Regulation of PDCD4 Promotes Proliferation, Angiogenesis and Tumorigenesis in Glioma Cells. *Front Cell Dev Biol*. 2020;8:593685.
36. Song S, Qiu X. LncRNA miR503HG inhibits epithelial-mesenchymal transition and angiogenesis in hepatocellular carcinoma by enhancing PDCD4 via regulation of miR-15b. *Dig Liver Dis*. 2021;53(1):107–16.
37. Zhao SF, Ye YX, Xu JD, et al. Long non-coding RNA KCNQ1OT1 increases the expression of PDCD4 by targeting miR-181a-5p, contributing to cardiomyocyte apoptosis in diabetic cardiomyopathy. *Acta Diabetol*. 2021;58(9):1251–67.